

Article

Influence of Heat Reflective Coating on the Cooling and Pavement Performance of Large Void Asphalt Pavement

Nanxiang Zheng, Junan Lei *, Shoubin Wang, Zhifeng Li and Xiaobao Chen

School of Highway, Chang'an University, Xi'an 710064, China; emailznx@163.com (N.Z.); 2016221152@chd.edu.cn (S.W.); 2019121201@chd.edu.cn (Z.L.); 2019121170@chd.edu.cn (X.C.)

* Correspondence: lja0604@chd.edu.cn

Received: 18 September 2020; Accepted: 3 November 2020; Published: 6 November 2020



Abstract: To reduce the temperature of asphalt pavement in summer, and alleviate the urban heat island effect, a comprehensive method of combining a heat reflective coating and large void asphalt pavement was proposed. Using the developed coating cooling test equipment, the cooling effect of the coating on a large void asphalt mixture was studied in six different proportions, four different colors, and four different dosages, and the durability of the coating was verified by abrasion tests. Finally, the best dosage of the coating was recommended through an adhesion test of the coating, and a water permeability and anti-skid performance test of the pavement. The results show that the reflectivity of the coating can be improved by adding functional fillers, of titanium dioxide and floating beads, into the coating. The order by reflectivity and cooling effect of the four color coatings was green > red > gray > blue, and the maximum cooling value of the green coating reached 9.7 °C. The cooling performance of the coating decreased with the increase of wear time, and the rate of decrease was fast, then slow, and finally tended to be stable after 20,000 times wear. The coating reduced the anti-skid performance and the water permeability coefficient of large void asphalt pavement, but still maintained a high level. The green coating with 15% titanium dioxide and 10% floating beads is recommended as the cooling coating for large void asphalt pavement, and its dosage should be controlled at about 0.4–0.8 kg/m².

Keywords: heat reflective coating; cooling performance; large void asphalt mixture; pavement performance

1. Introduction

Asphalt pavement has the advantages of low noise and comfortable driving, and is widely used in expressways and urban roads. However, black asphalt pavement has a very strong heat absorption property, especially under strong solar radiation in summer. Therefore, asphalt pavement easily produces rutting [1,2]. Furthermore, the heat absorbed by the pavement further aggravates the “heat island effect” of the city [3–5], and affects human health [6]. In order to reduce the temperature of asphalt pavement, several methods are being adopted currently, including thermal resistance pavement [7–9], water retention pavement [10–12], added phase change material pavement [13–15], and heat reflective coating pavement [16]. Among them, the heat reflective coating method is the most effective, and has been widely used. Zhu XY [17] applied a heat reflective coating to the sidewalk, which can reduce the temperature by 5.9 °C; Sha AM [18] designed a special solar heating reflective coating layer that can reduce the temperature by 10 °C; and Jiang L [19] designed a coating composed of a three-layer structure that can reduce the temperature by 13 °C. Yi Y [20] designed a red coating that can reduce the temperature by 10.2 °C.

Although the cooling effect of the heat reflective coating is preferable, it has an obvious influence on the anti-skid performance of the original pavement, and its wear resistance is poor. Cao XJ [21] applied a heat reflective coating to a dense asphalt pavement, and the anti-skid performance of the British pendulum number (BPN) decreased from 57 to 29 with the seriously worn coating. Zheng ML [22] applied a heat reflective coating to an AC-16 pavement at an amount of 0.6 kg/m^2 , and the BPN dropped from 68 to 31. However, large void asphalt pavement has the advantages of low thermal conductivity, good thermal insulation effect, and high anti-skid performance. The research of Hassn A [23] and Xie XG [24] showed that a large void mixture had a low specific heat capacity and thermal conductivity, which could be used to alleviate the urban heat island effect [25]. Therefore, it may be a good method to combine a heat reflective coating with large void asphalt pavement to give full play to their advantages. The coating is not only sprayed onto the road surface but also filled into the gaps, which can improve the wear resistance and durability of the coating, and meanwhile having little impact on the skid resistance of the original pavement, to ensure driving safety. This paper intends to study the application of heat reflective coatings on large void asphalt pavement for better cooling and pavement performance.

2. The Cooling Mechanism of Large Void Coated Pavement

The heat exchange of asphalt pavement is related to the natural environment. As shown in Figure 1 [26], the heat sources of the asphalt pavement mainly include direct solar radiation, scattering radiation, and atmospheric reverse radiation. The heat dissipation includes road reflection, heat convection, and heat conduction. All of these constitute the heat exchange between the asphalt pavement and the environment.

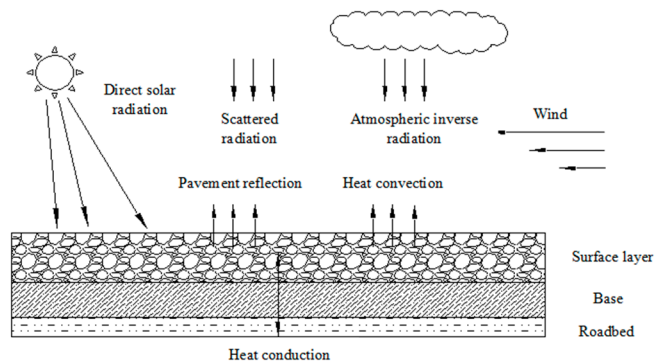


Figure 1. Thermal radiation characteristics of asphalt pavement.

To reduce the temperature, the fundamental method is to change the surface characteristics and heat transfer performance of the asphalt pavement, as shown in Figure 2, which is the composition of the large void coated pavement.

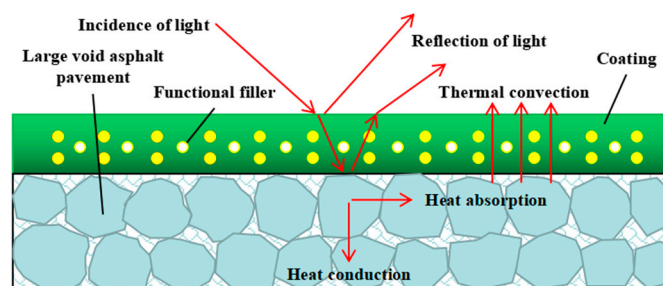


Figure 2. Cooling mechanism of large void coated pavement.

The cooling pavement is mainly composed of a heat reflective coating and a large void asphalt pavement. The use of a heat reflective coating can improve the reflection of the road surface to sunlight. The application of large void asphalt pavement can, not only reduce the thermal conductivity of the road and the heat conducted to the inside of the road surface, but also facilitate the convection of road heat and the air, and increase the heat dissipation capacity of the road surface. In this way, the comprehensive application of the coating and the large-void asphalt pavement can fully achieve the purpose of reducing the surface and internal temperature of the pavement.

3. Materials and Methods

3.1. Raw Materials

3.1.1. Raw Materials for Coating

The heat reflective coating material is mainly composed of three parts: matrix material, functional filler, and admixture, as shown in Figure 3.

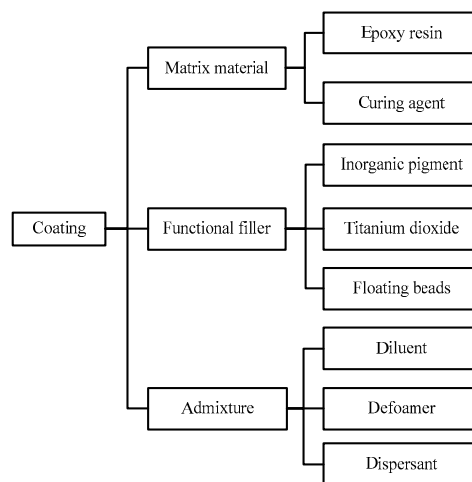


Figure 3. Composition of the coating material.

The matrix material plays a major role in the mechanical properties of the coating, and includes epoxy resin and curing agent. E-51 epoxy resin and 593 curing agent were selected for this study. E-51 epoxy resin is a kind of thermosetting polymer synthetic material, with a high epoxy value, low viscosity, and light color. Due to its advantages of high strength, good adhesion, corrosion resistance, and low shrinkage after curing, it is widely used in pavements and coatings. The 593 curing agent can react with epoxy resin at room temperature, which can accelerate the curing of the coating for the purpose of reopening traffic quickly.

Functional fillers include rutile titanium dioxide, floating beads, and inorganic pigments, as shown in Figure 4. Titanium dioxide has a large shading index and can improve the scattering ability of the coating to sunlight. The floating bead is a kind of fly ash hollow ball that can float on water. Its chemical composition mainly includes silica and aluminum oxide. It has the functions of wear resistance, heat insulation, and flame retardance. The pigment can adjust the color of the coating. Four colors of inorganic pigment, green, red, blue, and gray, were selected. The main chemical composition of the inorganic pigments is iron oxide.



Figure 4. Functional fillers: (a) Titanium dioxide; (b) Floating beads; (c) Inorganic color pigments.

The additives include diluent, defoamer, and dispersant, which can reduce the viscosity of the coating and improve its workability, eliminate bubbles, and disperse the fillers, respectively.

3.1.2. Ratio Design and Preparation of Coating

According to the different dosages of filler, six different coating ratios were designed, as shown in Table 1.

Table 1. Coating ratio design.

Coating Number	TiO ₂ Volume Ratio ¹ (%)	Dosage of Floating Beads ² (%)	Dosage of Pigment ³ (%)	Dosage of Dispersant ⁴ (%)	Dosage of Defoamer ⁴ (%)	Dosage of Curing Agent ² (%)	Dosage of Diluent ² (%)
1#	10	—	30	0.6	0.3	25	10–35
2#	15	—	30	0.6	0.3	25	10–35
3#	20	—	30	0.6	0.3	25	10–35
4#	15	10	30	0.6	0.3	25	10–35
5#	15	20	30	0.6	0.3	25	10–35
6#	15	30	30	0.6	0.3	25	10–35

¹ Titanium dioxide volume ratio = $\frac{\text{Titanium dioxide volume}}{\text{Titanium dioxide volume} + \text{Resin volume}} \times 100\%$; ² The dosages of floating beads, curing agent, and diluent are the mass percentage of epoxy resin; ³ The dosage of pigment is the mass percentage of titanium dioxide; ⁴ The dosages of dispersant and defoamer are the mass percentage of the coating.

The heat reflective coating was prepared according to the process shown in Figure 5.

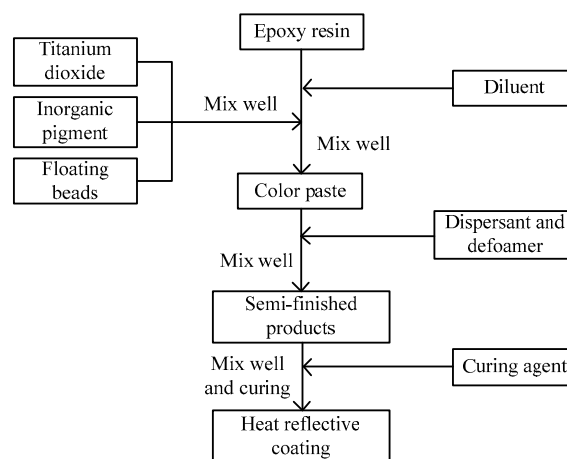


Figure 5. Flow chart of the heat reflective coating preparation.

The amount of each material was weighed, according to the designed ratio, before coating preparation. First, the diluent was added into the epoxy resin and stirred with a blender at a rate of 500–1000 r/min for 5–10 min. Second, the titanium dioxide, floating beads, and pigments were mixed together and added into the epoxy resin, and then the mixture was stirred at a rate of 1000–1500 r/min for 15–20 min. During the stirring, the dispersant and defoamer were added into the mixture, so we

could get the semi-finished coating product. Finally, the curing agent was added into the mixture and stirring continued for 10 min to obtain the finished coating.

3.1.3. Large Void Asphalt Mixture

OGFC-10 grade was selected to prepare the large void asphalt mixture, as shown in Figure 6. Shell high viscosity asphalt, basalt aggregate, and limestone powder were selected for the asphalt, coarse and fine aggregate, and mineral powder, respectively. Basalt aggregate has a high polishing value, and pavement constructed with it has a good skid resistance. A high viscosity asphalt can improve the road performance of the large void mixture. All materials had to meet the requirements of specification JTG F40-2004. The main technical indexes of the large void mixture, determined by the Marshall test, are shown in Table 2.

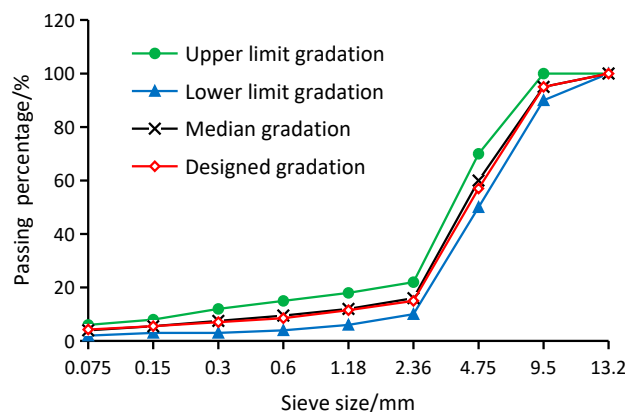


Figure 6. Gradation curve of the large void mixture.

Table 2. Main technical indexes of the large void mixture.

Technical Index	Result	Technical Index	Result
Gross bulk density (g/cm^3)	2.173	Maximum theoretical density (g/cm^3)	2.661
Air void (%)	18.3	VMA (%)	27.2
VFA (%)	32.6	OAC (%)	4.9
Marshall stability (kN)	6.3	Flow (mm)	2.3
Residual stability (%)	91.5	TSR (%)	89.1
Cantabro spatter loss (%)	7.5	Leakage loss (%)	0.02

3.2. Methods

3.2.1. Reflectivity Test of Coating

The No. 4 coatings of blue, gray, red, and green, and the No. 1–6 green coatings were prepared and sprayed on the surface of the specimen at the dosage of $0.6 \text{ kg}/\text{m}^2$. The specimen cut from the Marshall specimen was a quarter circle with a height of 2 cm and a radius of 5 cm, as shown in Figure 7a. Then, UV-Vis spectrophotometer (UV-2600, produced by Shimadzu, Kyoto, Japan) was used to test the reflectance of the coated and uncoated samples in 350–800 nm visible light, as shown in Figure 7b. Spectral reflectance measurements were performed according to ASTM E275 [27].

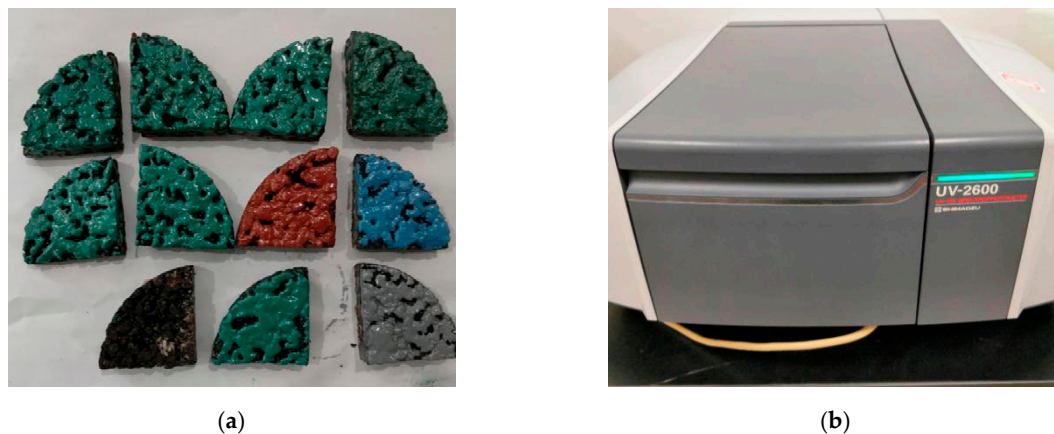


Figure 7. Coating reflectivity test: (a) Specimen; (b) UV-Vis spectrophotometer

3.2.2. Cooling Performance Test

A special piece of equipment was developed and used in the cooling test of the coating, as shown in Figure 8. It is mainly composed of a closed box, an iodine tungsten lamp, and a temperature collector.

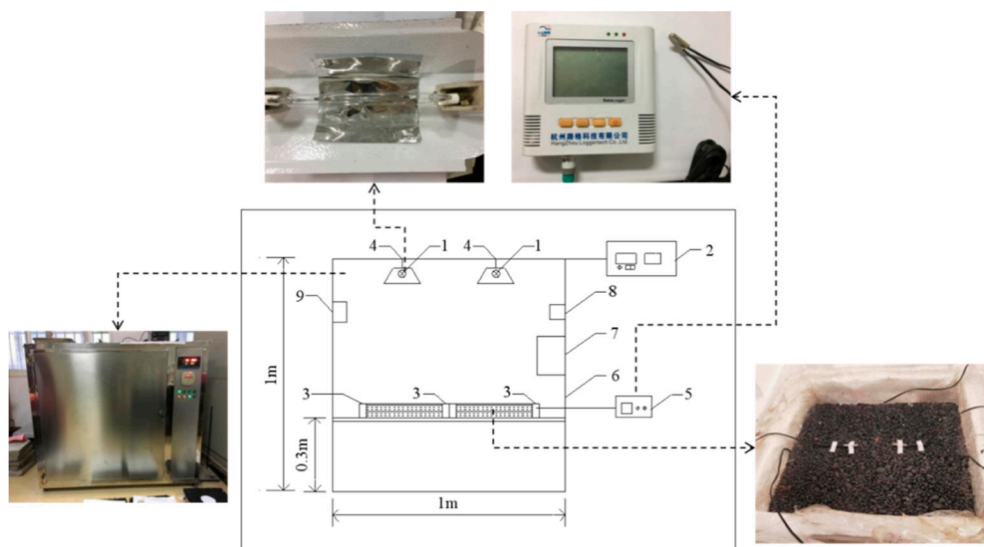


Figure 8. Coating cooling test equipment: 1-Iodine tungsten lamp; 2-Voltage regulator; 3-Thermal insulation layer; 4-Elevating pulley; 5-Temperature collector; 6-Closed box; 7-Heating device; 8-Stirring fan; 9-Humidity controller.

The test specimen was a rutting plate with a size of 30 cm × 30 cm × 5 cm. Before the test, No.1–6 green coatings (0.6 kg/m²), four colors of No. 4 coating (0.6 kg/m²), and No.5 green coating (0.2 kg/m², 0.4 kg/m², 0.6 kg/m², 0.8 kg/m²) were sprayed on the surface of the specimen. After the coating was fully cured, two small holes were drilled symmetrically at a distance of 2 cm from the top surface of the plate to embed the temperature sensor. At the same time, two temperature sensors were placed symmetrically at the top and bottom of the plate, and then the test piece was put into the heat insulation box of the equipment, as shown in Figure 8.

During the test, first, the equipment was opened, and meanwhile the initial temperature was set at 20 °C, for 4 h so that the temperature of each position of the rutting plate specimen was about 20 °C. Then, the iodine tungsten lamp was turned on to radiate for 5 h, the radiation intensity of the plate surface was controlled at about 850 W/m², and temperature data were recorded every 20 min with the

temperature collector. Finally, the collected temperature data were exported, and the average value of the two sensors data was taken as the final result.

3.2.3. Coating Abrasion Test

No. 1–6 green coatings were sprayed on half of the rutting plate at a dosage of 0.6 kg/m^2 . After the coating was completely cured, the abrasion test was carried out on the coated side with the rutting tester, in accordance with JTG E20-2011, as shown in Figure 9. The test temperature was set at $60 \text{ }^\circ\text{C}$, the wheel pressure was 0.7 Mpa , the wear width was 50 mm , and the wear rate was 42 times/min . After every $10,000$ wear cycles, the specimen was taken out for a cooling performance test, and the wear was stopped after $30,000$ times.

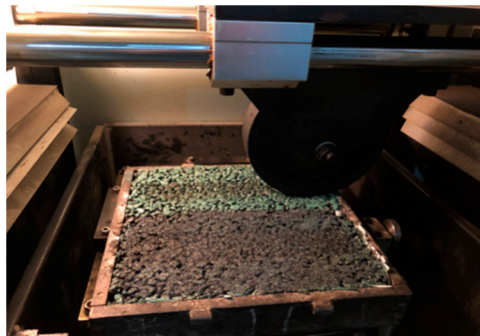


Figure 9. Abrasion test.

3.2.4. The Impact Tests of Coating on Pavement Service Performance

The prepared No. 4 green coating was sprayed on the surface of the rutting plate at the dosage of 0.2 kg/m^2 , 0.4 kg/m^2 , 0.6 kg/m^2 , 0.8 kg/m^2 , 1.0 kg/m^2 , and 1.2 kg/m^2 . After the coating was fully cured, the adhesion performance between the coating and the pavement, the water permeability, and skid resistance of the pavement were tested.

The adhesion performance was evaluated by a drawing test in accordance with ASTM D4541 [28]. The drawing head and the coating were bonded together before the coating was cured. After curing, the drawing test was conducted. The test temperature was $25 \text{ }^\circ\text{C}$, and the drawing rate was 0.1 MPa/s , as shown in Figure 10a.

The water permeability coefficient was tested with a water seepage meter, in accordance with JTG E60-2008, as shown in Figure 10b. The measuring cylinder was filled with water, and then the valve was opened. When the water level dropped to 100 mL , the stopwatch was pressed to count the time. When the water level dropped to 500 mL , the stopwatch was pressed again to record the required time. The water seepage coefficient was calculated according to Equation (1).

$$C_W = \frac{V_2 - V_1}{T_2 - T_1} \times 60, \quad (1)$$

where C_W is the permeability coefficient, mL/min ; V_1 is the water volume (mL) of the first timer, usually 100 mL ; V_2 is the water volume (mL) of the second timer, usually 500 mL ; T_1 is the time of the first timing (s); T_2 is the time of second timing (s).

The anti-skid performance was measured by a pendulum friction tester, as shown in Figure 10c. The anti-skid performance test was performed according to ASTM E275.

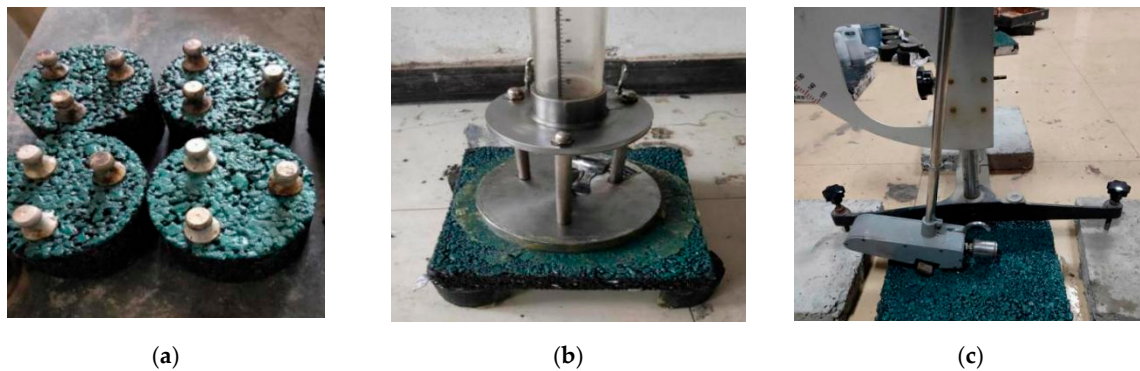


Figure 10. Influence of the coating on pavement performance test: (a) Drawing test; (b) Water penetration test; (c) Pendulum test.

4. Results and Discussion

4.1. Reflectivity of Coating

The reflectance test results of the coatings, with four different colors and different ratios of No. 1–6, are shown in Figure 11.

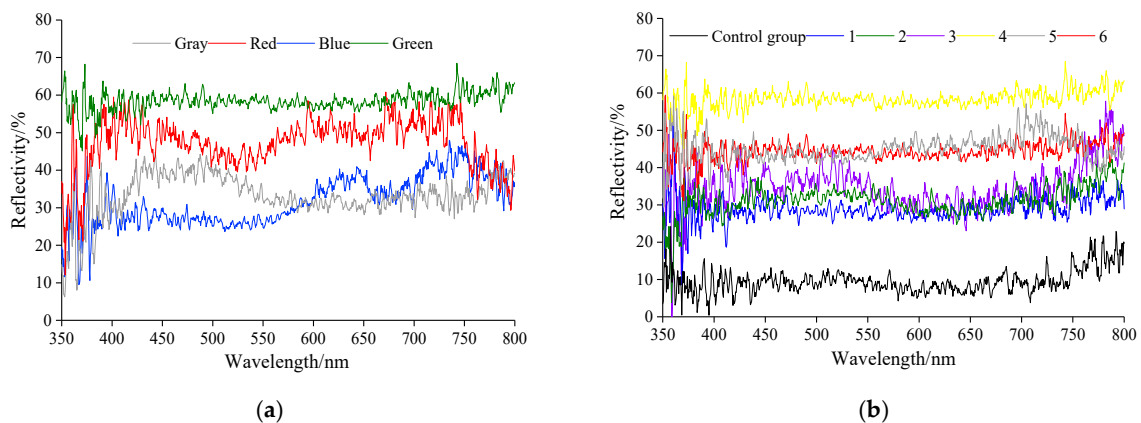


Figure 11. The reflectivity of the coating: (a) Reflectivity of different color coatings; (b) Reflectivity of coatings with different ratios.

From Figure 11a it can be seen that under the same ratio, the reflectivity of the green coating is the highest, with an average of about 60%, followed by the red coating, with an average of about 50%. When the wavelength is between 350 nm and 600 nm, the reflectance of the gray coating is higher than that of blue, and when the wavelength is between 600 nm and 800 nm, the reflectance of the blue coating is higher than that of gray. This may be because the reflection curve of gray without hue is relatively smooth, and the reflectivity of each wavelength is basically the same. The solar radiation is mainly concentrated in the visible region (400–760 nm), when the wavelength is 350–600 nm, it is close to the blue wavelength range (450–490 nm). The blue pigment absorbs other wavelengths and only reflects blue light, so the reflectivity is low. When the wavelength is 600–800 nm, it is all reflected, so the reflectivity increases.

From Figure 11b it can be seen that the reflectivity of the control group is only about 10%. While the reflectivity after the coating spraying was significantly increased, which shows that the coating could effectively increase the reflectivity of the specimen surface. The reflectivity of the coatings with different ratios was as follows: No. 4 > No. 5 > No. 6 > No. 3 > No. 2 > No. 1. Comparing No. 1, 2, and 3, it can be seen that the reflectivity of the coating increases with the volume concentration of TiO_2 . Comparing No. 2 and No. 5, it can be seen that the coating reflectivity can also be increased by floating beads.

Comparing No. 4–6, it can be seen that the reflectivity of the coating is reduced after more floating beads are added. This may be because there are too many floating beads to disperse evenly, and they will cover the titanium dioxide, resulting in a decrease of reflectivity.

4.2. Cooling Performance

4.2.1. Cooling Performance of Coatings with Different Ratios

The cooling performance of No. 1–6 coating is shown in Figure 12.

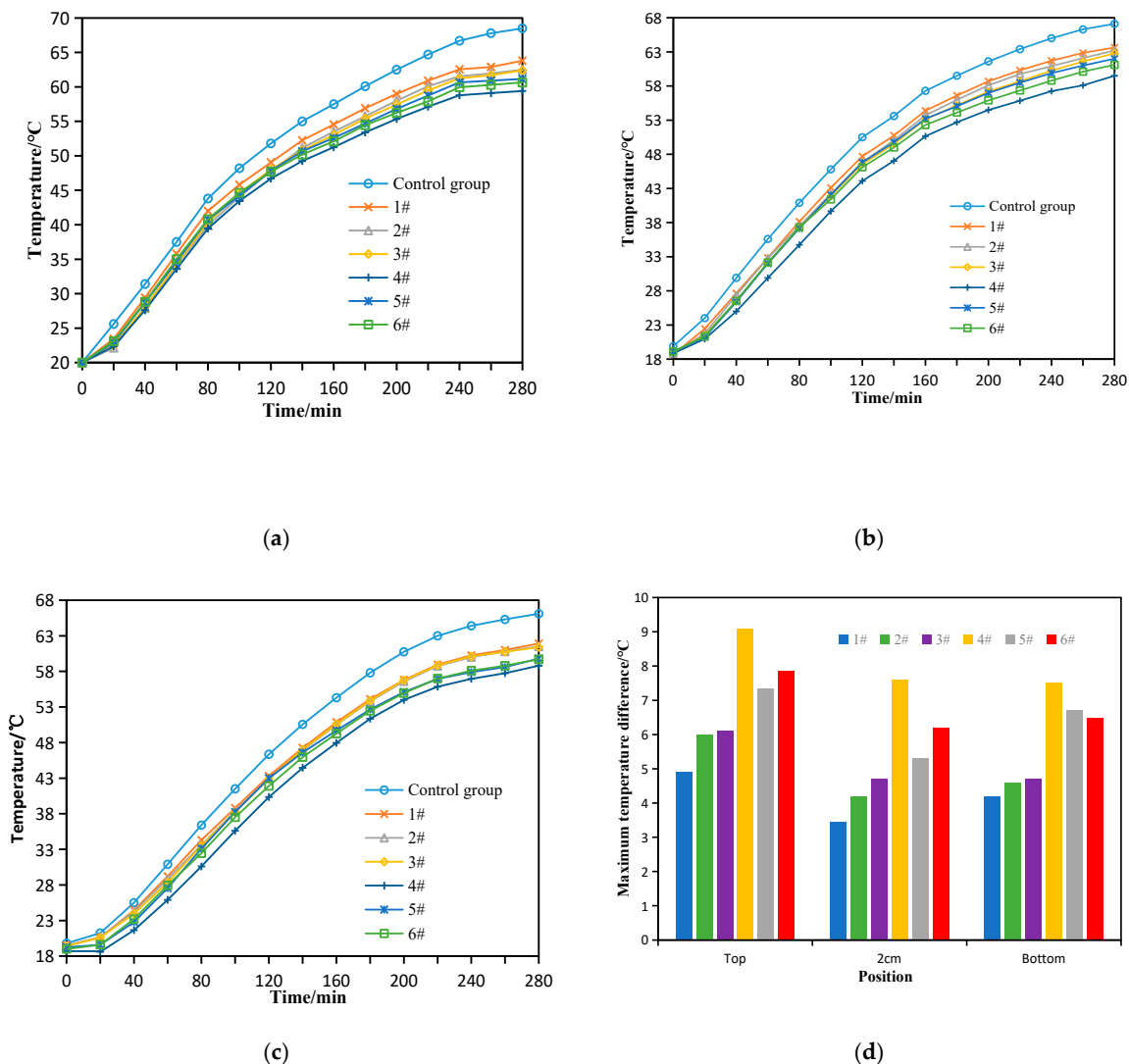


Figure 12. Cooling performance of coatings with different ratios: (a) The upper surface temperature of the specimen; (b) Temperature at 2 cm of the specimen; (c) Temperature at the bottom of the specimen; (d) Maximum temperature difference with the control group.

From Figure 12 it can be seen that compared with the uncoated specimens, the temperature of each layer of the coated specimens decreased to different degrees, and the cooling effect order was No. 4 > No. 6 > No. 5 > No. 3 > No. 2 > No. 1, and the cooling effect of No. 4 coated specimen was the best. This was mainly because the No. 4 coating contains more titanium dioxide, and an appropriate amount of floating beads, which can play an important role in heat reflection and heat insulation. The maximum temperature difference at different positions of the coated specimen was 4.9–9.1 °C on

the upper surface, 3.45–7.6 °C at 2 cm of the specimen, and 4.2–7.5 °C at the bottom of the specimen. This shows that the coating could effectively reduce the temperature at each height of the specimen.

4.2.2. Cooling Performance of Different Color Coatings

The cooling effect of the four color coatings of blue, gray, red, and green is shown in Figure 13.

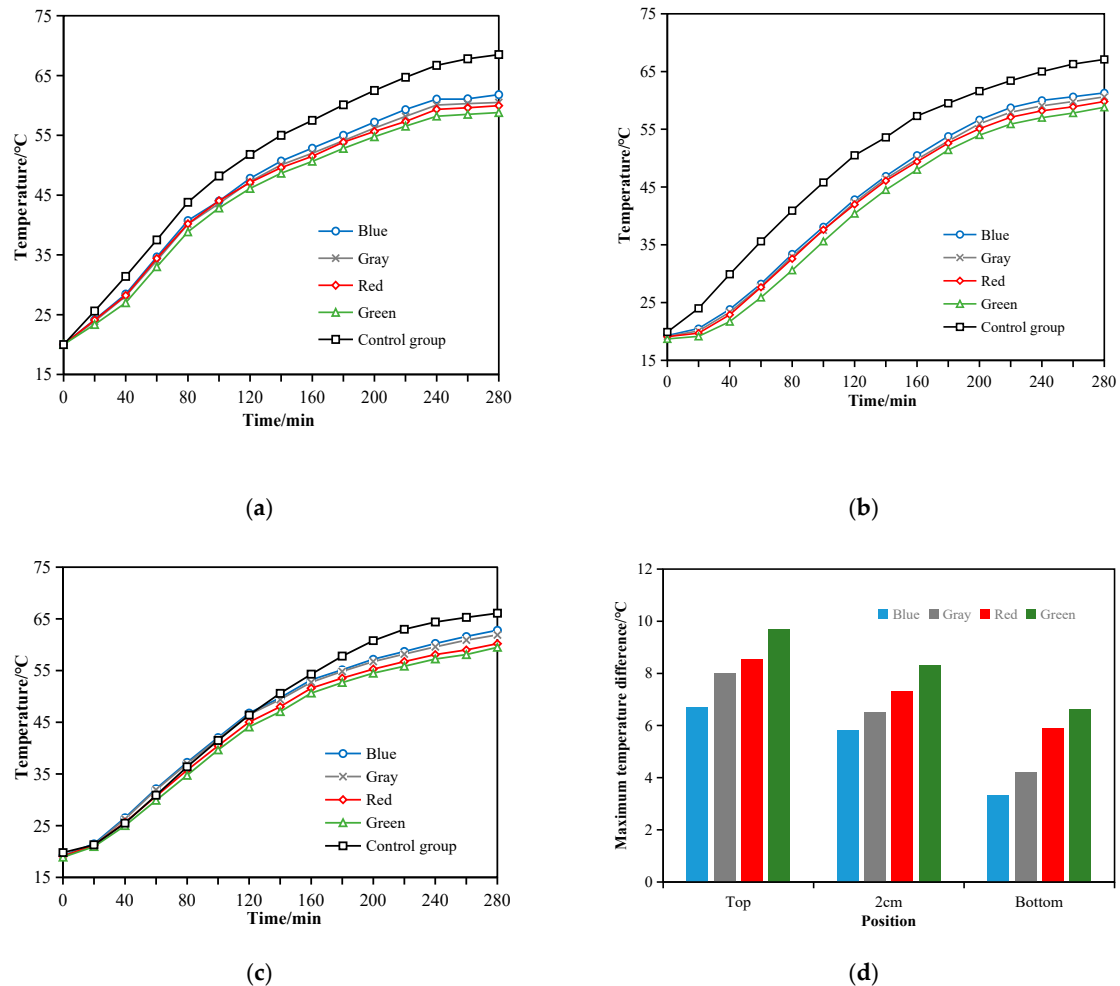


Figure 13. Cooling performance of different color coatings: (a) The upper surface temperature of the specimen; (b) Temperature at 2 cm of the specimen; (c) Temperature at the bottom of the specimen; (d) Maximum temperature difference with the control group.

From Figure 13 it can be seen that the temperatures of each layer of the four color coating specimens were in the order of blue > gray > red > green, which indicates that the cooling effect of green coating was the best, and that of the blue coating was the worst. This is mainly because the wavelength range of the iodine tungsten lamp is 190–1100 nm, which is close to the wavelength of the visible light (400–760 nm) of the sun. The lamp can simulate solar radiation very well. The green coating had the highest reflectivity, so the cooling effect was the best. Compared with the control groups, the maximum cooling value of green coating reached 9.7 °C, 8.3 °C, and 6.6 °C, respectively.

4.2.3. Cooling Performances of Coating with Different Dosages

The cooling performances of the coating with different dosages are shown in Figure 14.

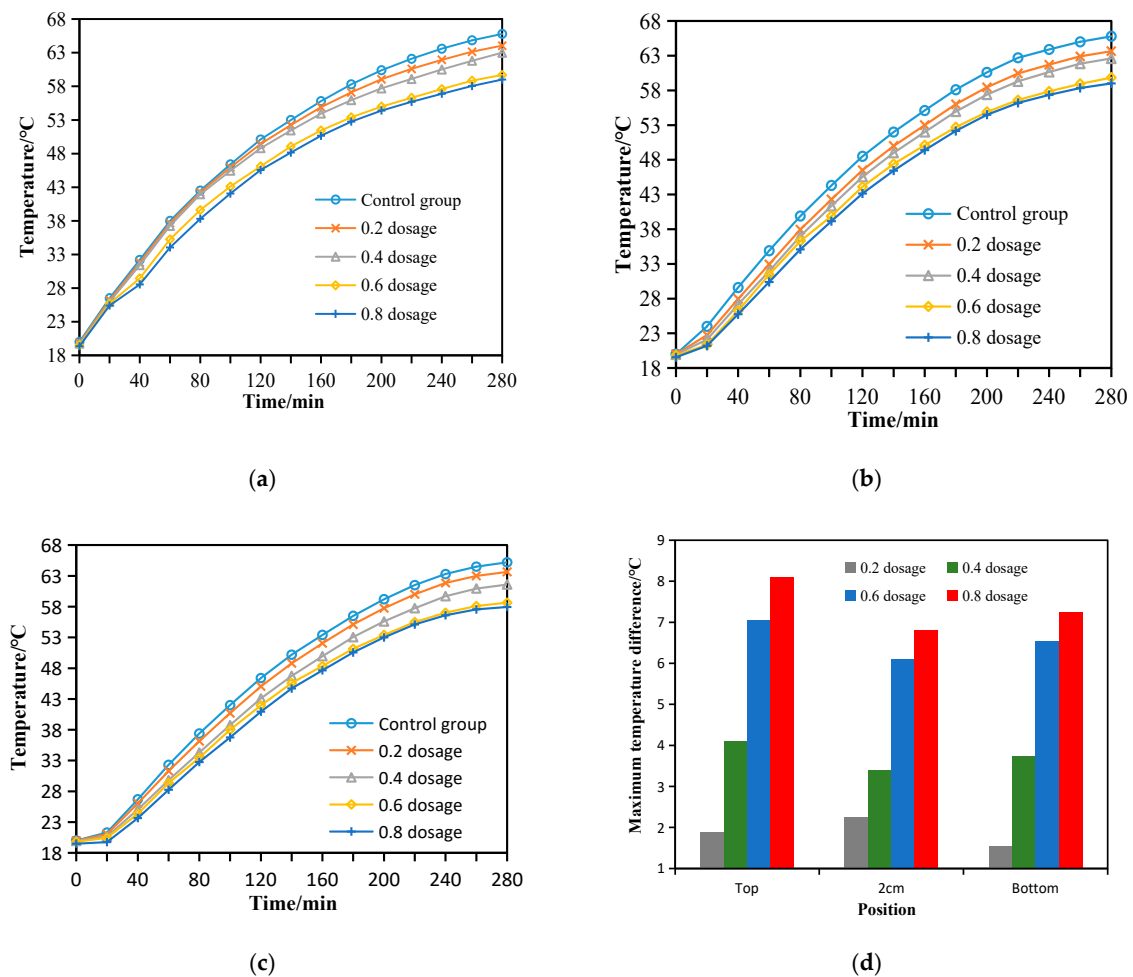


Figure 14. Cooling performance of different dosages of coating: (a) The upper surface temperature of the specimen; (b) Temperature at 2 cm of the specimen; (c) Temperature at the bottom of the specimen; (d) Maximum temperature difference with the control group.

From Figure 14 it can be seen that the temperature of the surface, at 2 cm, and bottom of the specimen decreases with the increase of the coating dosage. When the coating dosage was increased from 0.4 kg/m² to 0.6 kg/m², the maximum temperature difference changed the most. Compared with the control group, when the coating dosage was 0.8 kg/m², the temperature drop on the surface of the specimen was the largest, reaching 8.1 °C, 6.8 °C, and 7.3 °C, respectively.

4.3. Wear Performance

The wear of the coating specimen is shown in Figure 15, and the cooling performance test results of the coating after wear are shown in Figure 16.

From Figure 15 it can be seen that the wear makes the coating fall off from the surface of the mixture, and that the wear phenomenon becomes more obvious with the increase of wear time. However, some coatings in the voids of the mixture were not worn off, and could still play a cooling role. From Figure 16 it can be seen that when the number of wear increased, the maximum cooling value of each coating decreased. After 20,000 times of wear, the cooling performance tended to be stable. The cooling performance of No. 1–3 coating decreased by about 19%, and that of No. 5–6 coating decreased by 15% per 10,000 times of wear, which indicates that the wear resistance of the coating can be improved by adding floating beads.

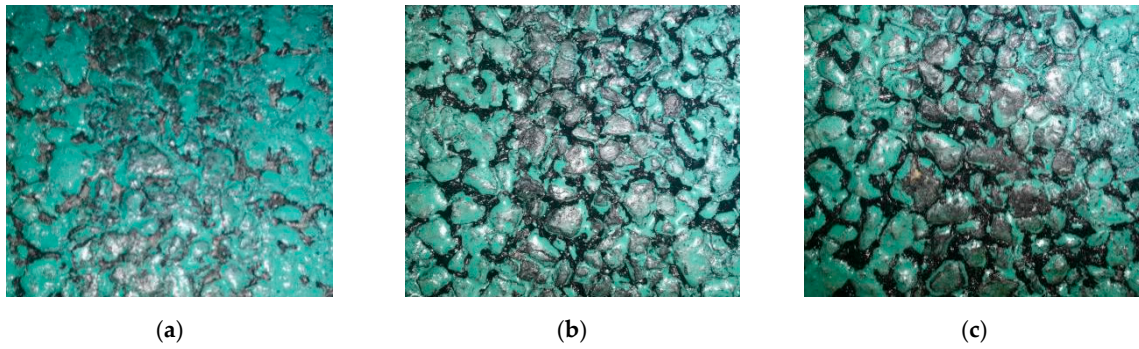


Figure 15. Coating after different wear times: (a) 10,000 times of wear; (b) 20,000 times of wear; (c) 30,000 times of wear.

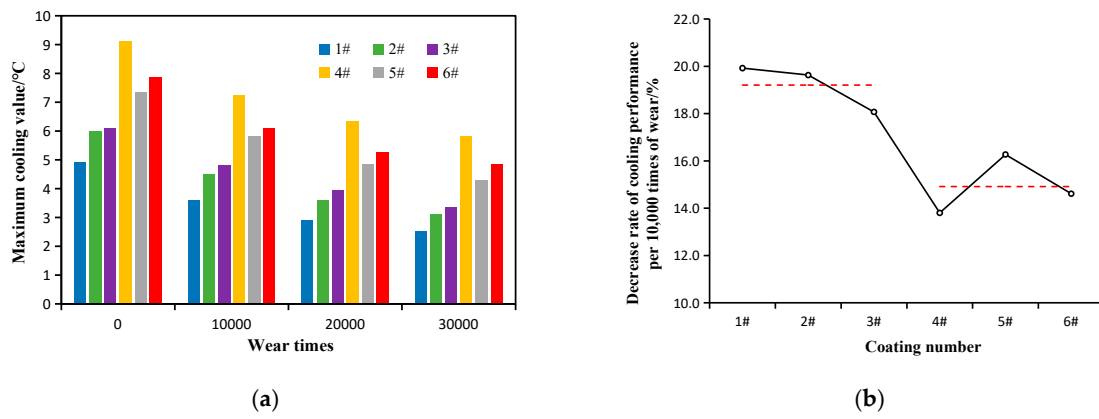


Figure 16. Effect of wear on cooling performance: (a) The maximum cooling value of the coating after different wear times; (b) Decrease rate of cooling performance of coating per 10,000 times of wear.

4.4. Influence of Coating on Pavement Performance

The influence of the coating on pavement performance of the mixture is shown in Figure 17.

From Figure 17 it can be seen that the adhesion strength increased at first, and then decreased with the increase of the coating dosage, reaching the maximum value of 1.65 MPa at about 0.6 kg/m². The anti-skid performance and water permeability coefficient of the mixture both decreased with the increase of the coating dosage, but still maintained a high level. To ensure driving safety, the dosage of coating should be controlled at about 0.4–0.8 kg/m².

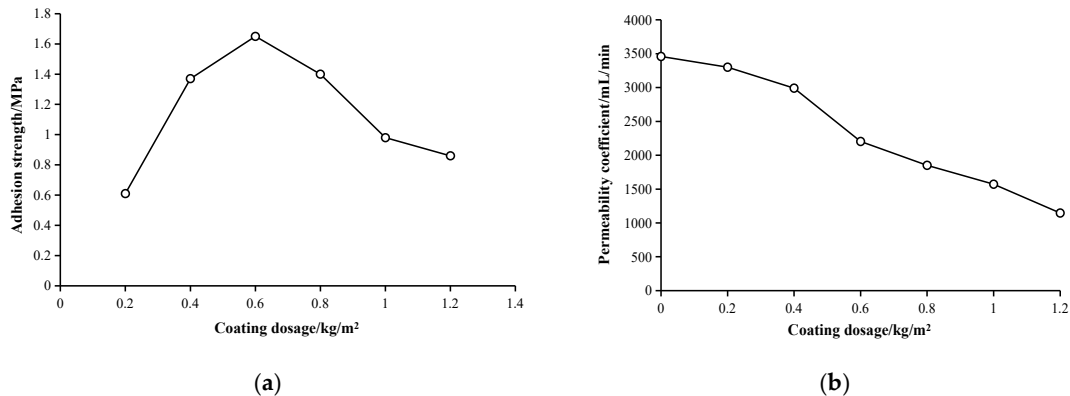
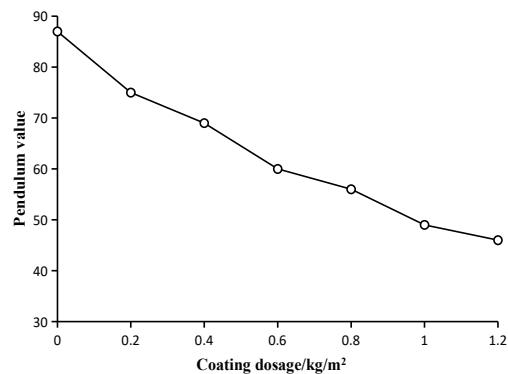


Figure 17. Cont.



(c)

Figure 17. Effect of the coating on pavement performance of the mixture: (a) Adhesion strength between coating and pavement; (b) Effect of coating on seepage performance of the mixture; (c) Effect of the coating on the skid resistance of the mixture

5. Conclusions

The following conclusions were obtained from the results of this study:

- Both titanium dioxide and floating beads can improve the reflectivity of the coating, and the reflectivity is proportional to the dosage of titanium dioxide.
- The order of reflectivity and cooling effect of the four color coatings was green > red > gray > blue. The green coating is recommended, and its maximum cooling value can reach 9.7 °C
- The cooling performance of the coating with 15% titanium dioxide and 10% floating beads was the best, and the higher dosage, the better the cooling effect. The cooling performance decreased with the increase of wear time and tended to be stable after 20,000 times of wear.
- The adhesion strength between the coating and pavement reached the maximum value of 1.65 MPa when the dosage of coating was 0.6 kg/m². The skid resistance and seepage coefficient of pavement decreased with the increase of coating dosage, but still maintained a high level.
- The green coating with 15% titanium dioxide and 10% floating beads is recommended as the cooling coating of large void asphalt pavement, and its dosage should be controlled at about 0.4–0.8 kg/m².

Author Contributions: Conceptualization, J.L.; data curation, X.C.; investigation, Z.L.; methodology, S.W.; project administration, N.Z.; writing—original draft, J.L.; writing—review & editing, J.L. All authors have read and agreed to the published version of the manuscript.

Funding: The research was funded by the scientific project from Longgang District Transportation Bureau of Shenzhen (No. 0722-1661-FE540SZB).

Acknowledgments: We are grateful for the support of Longgang District Transportation Bureau of Shenzhen.

Conflicts of Interest: The authors declare no conflict of interest.

References

1. Ji, X.P.; Zheng, N.X.; Hou, Y.Q.; Niu, S.S. Application of Asphalt Mixture Shear Strength to Evaluate Pavement Rutting with Accelerated Loading Facility. *Constr. Build. Mater.* **2013**, *41*, 1–8. [[CrossRef](#)]
2. Guo, R.; Nian, T.F.; Zhou, F. Analysis of factors that influence anti-rutting performance of asphalt pavement. *Constr. Build. Mater.* **2020**, *254*. [[CrossRef](#)]
3. Mohajerani, A.; Bakaric, J.; Jeffrey-Bailey, T. The urban heat island effect, its causes, and mitigation, with reference to the thermal properties of asphalt concrete. *J. Environ. Manag.* **2017**, *197*, 522–538. [[CrossRef](#)] [[PubMed](#)]
4. Deilami, K.; Kamruzzaman, M.; Liu, Y. Urban heat island effect: A systematic review of spatio-temporal factors, data, methods, and mitigation measures. *Int. J. Appl. Earth. Obs. Geoinf.* **2018**, *67*, 30–42. [[CrossRef](#)]

5. Yang, H.L.; Yang, K.; Miao, Y.H.; Wang, L.B.; Ye, C. Comparison of Potential Contribution of Typical Pavement Materials to Heat Island Effect. *Sustainability* **2020**, *12*, 4752. [[CrossRef](#)]
6. Tan, J.G.; Zheng, Y.F.; Tang, X.; Guo, C.Y.; Li, L.P.; Song, G.X.; Zhen, X.R.; Yuan, D.; Li, F.R.; Chen, H. The Urban Heat Island and Its Impact on Heat Waves and Human Health in Shanghai. *Int. J. Biometeorol.* **2010**, *54*, 75–84. [[CrossRef](#)]
7. Wang, C.H.; Fu, H.; Fan, Z.T.; Li, T.Y. Utilization and properties of road thermal resistance aggregates into asphalt mixture. *Constr. Build. Mater.* **2019**, *208*, 87–101. [[CrossRef](#)]
8. Li, C.X.; Yang, J.H.; Zhang, K. Thermal insulation and cooling characteristics of thermal resistance asphalt mixture and evaluation of its pavement performance. *J. Xi'an Univ. Arch. Tech.* **2019**, *51*, 375–382. (In Chinese)
9. Gao, Z.W.; Liu, L.Q.; Xiao, X.D.; Wang, C.H.; Mu, K. Research progress of thermal resistance asphalt mixture. *J. Chang'an Univ.* **2020**, *40*, 125–134. (In Chinese)
10. Qin, Y.H. A Review on the Development of Cool Pavements to Mitigate Urban Heat Island Effect. *Renew. Sust. Energ. Rev.* **2015**, *52*, 445–459. [[CrossRef](#)]
11. Nakayama, T.; Fujita, T. Cooling Effect of Water-Holding Pavements Made of New Materials on Water and Heat Budgets in Urban Areas. *Landsc. Urban. Plan.* **2010**, *96*, 57–67. [[CrossRef](#)]
12. Li, H.; Harvey, J.; Ge, Z.S. Experimental Investigation on Evaporation Rate for Enhancing Evaporative Cooling Effect of Permeable Pavement Materials. *Constr. Build. Mater.* **2014**, *65*, 367–375. [[CrossRef](#)]
13. Ma, B.A.; Wang, S.S.; Li, J. Study on Application of PCM in Asphalt Mixture. *Adv. Mat. Res.* **2011**, *168*, 2625–2630. [[CrossRef](#)]
14. Chen, M.Z.; Wan, L.; Lin, J.T. Effect of Phase-Change Materials on Thermal and Mechanical Properties of Asphalt Mixtures. *J. Test. Eval.* **2012**, *40*, 746–753. [[CrossRef](#)]
15. Anupam, B.R.; Sahoo, U.C.; Rath, P. Phase change materials for pavement applications: A review. *Constr. Build. Mater.* **2020**, *247*, 118553. [[CrossRef](#)]
16. Pan, S.P.; Sun, B.X.; Zhan, P.M.; Chen, X.; Miao, J.Q. Overview of Studies on Pavement Cooling Mechanism and Its Influencing Factors Based on Reflectance. *J. Highw. Transp. Res. Dev.* **2019**, *36*, 14–23. (In Chinese)
17. Zhu, X.Y.; Yu, Y.; Chen, L.; Zhang, D.W. Solar Heat Reflective Coating for Sidewalks Considering Cooling Effect, Anti-Skid Performance, and Human Comfort. *J. Test. Eval.* **2020**, *48*, 2028–2039. [[CrossRef](#)]
18. Sha, A.M.; Liu, Z.Z.; Tang, K.; Li, P.Y. Solar heating reflective coating layer (SHRCL) to cool the asphalt pavement surface. *Constr. Build. Mater.* **2017**, *139*, 355–364. [[CrossRef](#)]
19. Jiang, L.; Wang, L.C.; Wang, S.Y. A novel solar reflective coating with functional gradient multilayer structure for cooling asphalt pavements. *Constr. Build. Mater.* **2019**, *210*, 13–21. [[CrossRef](#)]
20. Yi, Y.; Jiang, Y.J.; Li, Q.L.; Deng, C.Q.; Ji, X.P.; Xue, J.S. Development of Super Road Heat-Reflective Coating and Its Field Application. *Coatings* **2019**, *9*, 802. [[CrossRef](#)]
21. Cao, X.J.; Tang, B.M.; Zhu, H.Z.; Zhang, A.M.; Chen, S.M. Cooling Principle Analyses and Performance Evaluation of Heat-Reflective Coating for Asphalt Pavement. *J. Mater. Civil Eng.* **2011**, *23*, 1067–1075. [[CrossRef](#)]
22. Zheng, M.L.; He, L.T.; Gao, X.; Wang, F.; Cheng, C. Analysis of heat-reflective coating property for asphalt pavement based on cooling function. *J. Traffic Transp. Eng.* **2013**, *13*, 10–16. (In Chinese)
23. Hassn, A.; Aboufoul, M.; Wu, Y.; Dawson, A.; Garcia, A. Effect of air voids content on thermal properties of asphalt mixtures. *Constr. Build. Mater.* **2016**, *115*, 327–335. [[CrossRef](#)]
24. Xie, X.G.; Wang, L.; Zhang, X. Research on Ecological Efficiency of Asphalt Mixture with Different Porosities. *J. Highw. Transp. Res. Dev.* **2015**, *32*, 20–25.
25. Stempihar, J.J.; Pourshams-Manzouri, T.; Kaloush, K.E.; Rodezno, M.C. Porous Asphalt Pavement Temperature Effects for Urban Heat Island Analysis. *Transp. Res. Rec.* **2012**, *2293*, 123–130. [[CrossRef](#)]
26. Zheng, M.L.; Tian, Y.J.; He, L.T. Analysis on Environmental Thermal Effect of Functionally Graded Nanocomposite Heat Reflective Coatings for Asphalt Pavement. *Coatings* **2019**, *9*, 178. [[CrossRef](#)]
27. ASTM International. *ASTM E275-08/13R-Standard Practice for Describing and Measuring Performance of Ultraviolet and Visible Spectrophotometers*; ASTM International: West Conshohocken, PA, USA, 2013.

28. ASTM International. *ASTM D4541-17-Standard Test Method for Pull-off Strength of Coatings Using Portable Adhesion Testers*; ASTM International: West Conshohocken, PA, USA, 2017.

Publisher's Note: MDPI stays neutral with regard to jurisdictional claims in published maps and institutional affiliations.



© 2020 by the authors. Licensee MDPI, Basel, Switzerland. This article is an open access article distributed under the terms and conditions of the Creative Commons Attribution (CC BY) license (<http://creativecommons.org/licenses/by/4.0/>).